Observation of a hydrogen-induced shape resonance on Pt/LTL catalysts and its relation with support acidity/alkalinity

B.L. Mojet [a,*], D.E. Ramaker [b], J.T. Miller [c] and D.C. Koningsberger [a,**]

[a] *Department of Inorganic Chemistry and Catalysis, Debye Institute, Utrecht University, PO Box 80083, 3508 TB Utrecht, The Netherlands*
[b] *Department of Chemistry and Material Science Institute, George Washington University, Washington DC, USA*
[c] *Amoco Research Center, E-1F, 150 W Warrenville RD, Naperville, IL 606563, USA*

Received 12 April 1999; accepted 20 July 1999

A novel analysis method of the platinum L_3 and L_2 X-ray absorption edges of Pt/LTL catalysts indicates that chemisorbed hydrogen induces an antibonding resonance state just above the Fermi level at the Pt L_3 edge. The difference in energy of this antibonding state (E_{res}) with respect to the Fermi level is strongly influenced by the acidity/alkalinity of the LTL support: E_{res} decreases with increasing alkalinity. The decrease in E_{res} can also be correlated with the decrease of the neopentane hydrogenolysis turnover frequency of Pt/LTL with increasing support alkalinity. These results provide the most direct experimental evidence that the support acidity/alkalinity alters the actual chemical bond between the surface platinum atoms and the reacting molecule.

Keywords: shape resonance, metal–support interaction, XAFS spectroscopy, Pt/LTL, Pt–H bonding, support acidity/alkalinity

1. Introduction

The mechanism of the metal–support interaction and, more precisely, how the electronic structure of the catalytically active surface metal atoms is altered by the support is still not being solved in the literature. However, the effects of the metal–support interaction on the catalytic properties of noble metal particles have been found and discussed by many authors [1–8]. The formation of a metal–proton adduct has been proposed to account for electron-deficient metal particles [9]. The electron deficiency was derived from XPS data collected on Pd metal particles dispersed in acidic zeolites [10]. The proton was proposed to be delocalised over the metal particle thereby withdrawing electron density from the surface atoms. However, such adducts cannot account for an increase in electron density for metal particles on alkaline supports. In another model, the electronegativity of the support oxygen atoms was suggested to decrease with increasing zeolite alkalinity [11–13]. Charge transfer between the support oxygen atoms and the close by metal particles was thought to cause higher electron density on the metal particles in alkaline zeolites. A third model is based on the polarisation of a small metal cluster by nearby cations [14,15]. Calculations indicated that metal atoms near cations attract electrons, thus resulting in electron-deficient metal atoms situated at the opposite side of the cluster. In this model, there is no net change in electron density of the cluster.

From this summary it is clear that the mechanism of the metal–support interaction and more precisely how the electronic structure of the catalytically active surface metal atoms is altered by the support is still unknown. To understand the interaction involved, we have investigated the effect of the support on the X-ray absorption edge of very small platinum particles in zeolite LTL with and without adsorbed hydrogen, a reactant used in many catalytic reactions.

It is well known that hydrogen significantly affects the near-edge region of the Pt and Pd $L_{2,3}$ X-ray absorption edges. Mansour et al. [16] observed that the areas of the Pt $L_{2,3}$ white lines increased with exposure to H_2 in comparison to Pt foil and developed a quantitative technique for determination of the number of unoccupied d-electron states. Lytle et al. [17] observed significant changes in white line shape and intensity of the Pt $L_{2,3}$ edges for Pt/SiO_2 heated in H_2 vs. He and as a function of temperature. Samant and Boudart [18] noted similar changes in H–Pt vs. He/Pt clusters dispersed in Y zeolite. Vaarkamp et al. [19] showed an effect of interfacial hydrogen between the platinum cluster and the support on the Pt $L_{2,3}$ white line in an attempt to explain the difference in reactivity of γ-Al_2O_3-supported Pt particles as a function of reduction temperature. By comparing experimental data with multiple scattering calculations, Soldatov et al. [20] found that H introduced a multiple scattering state in the Pd L_3 white lines of $PdH_{0.6}$. Asakura et al. [21] and Reifsnyder et al. [22] suggested a new Pt–H resonance state visible in XAFS data after hydrogen adsorption on supported Pt particles. Finally, Boyanov et al. [23] observed two features in the H/Pt minus Pt foil $L_{2,3}$ difference spectra of Pt clusters

* Current address: Schuit Institute of Catalysis, Eindhoven University of Technology, PO Box 523, 5600 MB Eindhoven, The Netherlands.
** To whom correspondence should be addressed.

supported on zeolite Y and interpreted them as spin–orbit doublets.

This paper utilises a new analysis method [24] of the L_3 and L_2 X-ray absorption edges of small platinum particles dispersed in LTL zeolite. The new white line analysis method allows the isolation of an antibonding resonance state present above the Fermi level at the L_3 edge. This antibonding state originates from chemisorption of hydrogen on the surface atoms of the platinum particles. The difference in energy of the antibonding state with respect to the Fermi level (E_{res}) decreases with increasing alkalinity of the LTL zeolite support, implying a decrease in the strength of the Pt–H bond. The results will be discussed in terms of a direct influence of the support on the electronic structure of the platinum surface atoms thereby affecting their catalytic properties.

2. Experimental

2.1. Catalyst preparation

The acidity/alkalinity of the LTL zeolite supports was varied by either impregnating a commercial K-LTL zeolite with KNO_3 or exchanging it with NH_4NO_3 to give K/Al ratios ranging from 0.63 to 1.25 (see table 2). Each LTL zeolite was calcined at 225 °C. Platinum (1 wt%) was added by incipient wetness impregnation using an aqueous solution of $[Pt(NH_3)_4](NO_3)_2$ followed by drying at 120 °C. The catalysts are designated Pt/LTL(x) with x representing the K/Al molar ratio.

2.2. Neopentane hydrogenolysis

Neopentane hydrogenolysis was carried out in a fixed-bed reactor using 1 vol% neopentane in H_2. The catalysts were pre-reduced in H_2 at the reaction temperature and conversion was adjusted to values between 0.5 and 2.0% by varying space velocity. The turnover frequency (TOF) is calculated based on the dispersion values obtained by chemisorption [25].

2.3. XAFS data collection

The X-ray absorption spectra of the Pt L_3 and L_2 edge were taken at the SRS (Daresbury) Wiggler Station 9.2, using a Si(220) double-crystal monochromator. The measurements were done in transmission mode using ion chambers filled with Ar to have an X-ray absorbance of 20% in the first and of 80% in the second ion chamber. The monochromator was detuned to 50% maximum intensity to avoid higher harmonics present in the X-ray beam.

Samples were pressed into self-supporting wafers (calculated to have an absorbance of 2.5) and placed in a controlled atmosphere cell [26]. Spectra were recorded at liquid-nitrogen temperature for the Pt/LTL samples after reduction in H_2 at 300 °C (samples further denoted by H–Pt/LTL) and subsequent treatment in a helium flow for 1 h at 300 °C to remove chemisorbed hydrogen (samples further denoted by Pt/LTL).

2.4. XAFS data analysis

The final XAFS spectrum was obtained by averaging 3–4 scans. The pre-edge background was approximated by a modified Victoreen curve [19], the background was subtracted using cubic spline routines [27]. Spectra were normalised by dividing the absorption intensity by the height of the absorption edge at 50 eV above the edge [19].

3. Isolation of the Pt–H antibonding shape resonance

Hydrogen chemisorption induces a bonding and an antibonding orbital, as reported by Hammer et al. [28] (see figure 1). The partially occupied "dangling" platinum surface orbitals form a bond with the hydrogen 1s orbital producing the bonding and antibonding Pt–H orbitals. The antibonding state can be viewed as a localised state degenerate with a continuum state, here described by the Pt–H EXAFS final state wavefunction. The outgoing electron will reside temporarily in the potential well determined by the AS state and can escape undergoing a resonance with the Pt–H EXAFS final state wavefunction. This one electron process causes a shape resonance with the well-known Fano-like resonance line shape. Its effect on the scattering cross section $\sigma(E)$ can be related to an EXAFS function $\chi(E)$ via the normal expression $\sigma(E) = \mu(E)(1 + \chi(E))$. It can be shown [24] that

$$\chi(E) = \frac{1}{k} \cdot A \sin\Phi \cdot \frac{1 - q\varepsilon}{1 + \varepsilon^2}, \tag{1}$$

with A an amplitude factor, $q = \cot\Phi$ and $\varepsilon = (E - E_{\text{res}})/\Gamma$. Φ can be related to the usual total phase found in EXAFS containing the $2kr$ term and the phase from the absorber and back-scatterer. ε is the normalised energy scale relative to the resonance energy (E_{res}), whereby Γ represents the resonance width. A fit to the experimentally observed AS line shape gives values for E_{res}, Γ, A and Φ.

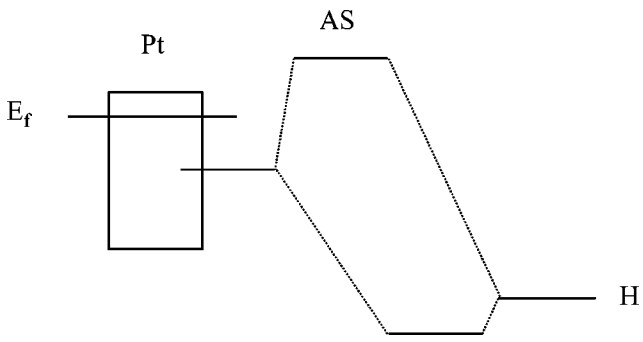

Figure 1. MO picture showing formation of bonding and antibonding orbitals derived form a surface Pt orbital and the H 1s orbital.

The Pt–H antibonding shape resonance can be isolated from the experimental data using a new analysis method of the L_2 and L_3 white line areas, which is based upon several theoretical concepts as previously described [24]. Table 1 summarises the important contributions that will be visible in the four X-ray absorption edges of platinum in Pt/LTL catalysts, based on the assumptions and theory described in [24]. The L_2 edge spectrum for "clean" Pt clusters can be used as the reference (REF), since this spectrum arises from the "free" atom absorption and the EXAFS contributions. The L_3 spectrum of the clean Pt cluster contains in addition the electronic (empty valence band: ΔVB) contribution [24]. The L_2 spectrum for the H–Pt sample is different from the REF spectrum, because of changes in geometry of the cluster induced by chemisorption of hydrogen (changes in XAFS scattering: ΔXAFS). The Pt–H bonding orbital is primarily localised on the H atom, and the antibonding state (AS) is localised more on the surface Pt atoms, causing the $5d_{3/2}$ component of the AS state to shift below the Fermi level. Therefore, the transition of outgoing electron to the empty antibonding orbital should be evident only in the near-edge spectrum of the H–Pt L_3 X-ray absorption edge. Finally, the L_3 spectrum for the H–Pt sample contains both the geometric (ΔXAFS) and electronic (ΔVB+AS) changes from the reference.

Before the different contributions (ΔVB, ΔXAFS, AS) can be separated from the X-ray absorption spectra, the edges have to be aligned in order to account for initial and final state effects. The alignment procedure is extensively discussed in [24].

4. Results

Table 2 reports the neopentane hydrogenolysis TOF for the catalysts. A gradual decrease in TOF is observed with increasing support alkalinity (i.e., higher K/Al ratio), as reported earlier for Pt/LTL, Pd/LTL and Pt/SiO_2 catalysts [25,29].

Table 1
Main information present in the Pt L_3 and L_2 near-edge spectra.

Sample	L_3 edge	L_2 edge
H–Pt	REF + ΔXAFS + ΔVB + AS	REF + ΔXAFS
Pt	REF + ΔVB	REF

Table 2
Elemental composition, dispersion, EXAFS coordination numbers and neopentane TOF of Pt/LTL catalysts.

Catalyst	K (wt%)	Al (wt%)	H/Pt	N (EXAFS)[a]	Neopentane TOF[b]
H–Pt/LTL(0.63)	8.3	9.5	0.53	3.7	1.8×10^{-1}
H–Pt/LTL(0.96)	11.8	8.5	0.89	4.2	3.7×10^{-2}
H–Pt/LTL(1.25)	15.9	8.8	0.88	2.3	4.9×10^{-5}

[a] See also [30].
[b] Reaction temperature: 350 °C [8].

The full analysis of the EXAFS data of the Pt/LTL catalysts is presented in [30]. The analysis showed that the first-shell Pt–Pt coordination number for all three catalysts is smaller than 4.5 (see table 2), implying platinum particles consisting of an average of 4–5 atoms. The structure of the platinum particles is not largely influenced by He treatment.

Figure 2(a) displays the Pt L_2 and L_3 X-ray absorption edges for H–Pt/LTL(0.96) (solid line) and Pt/LTL(0.96) (dashed line) after the novel alignment procedure. It can be seen that the presence of hydrogen chemisorption induces large changes in shape, intensity and position of the white lines of both edges, as previously observed [16–19]. Furthermore, figure 2(b) shows that the near-edge platinum data of the H–Pt/LTL catalysts are also largely affected by the acidity/alkalinity of the LTL support. The influence of the support on shape, intensity and position of the near-edge features is different for all three samples.

The Pt–H antibonding shape resonace (AS) can be obtained by subtracting $\Delta L_2 = L_2$(H–Pt) – L_2(Pt) from $\Delta L_3 = L_3$(H–Pt) – L_3(Pt). Figure 3 shows this antibonding resonance for the acidic Pt/LTL(0.63) and the basic Pt/LTL(1.25). Equation (1) was used in a non-linear least squares fit to the experimental AS line shapes. Besides the resonance parameters, a Gaussian broadening of 5 eV was added to account for the experimental resolution. Since q and Γ are strongly interdependent and the width is quite uncertain because of the experimental broadening, q and E_{res} are coupled utilising the relation $q = \alpha + \beta E_{\mathrm{res}}$. The line shapes of all three samples were then fitted simultaneously with a total of 11 parameters, i.e., E_{res}, Γ, and A for each resonance, plus α and β which are given in table 3. The dramatic reversal in line shape of the shape resonance is easily reproduced by the expression in equation (1) (see dotted lines in figure 3(b)).

5. Discussion

The Pt–H antibonding state shape resonance (AS) clearly shows a relationship between the catalytic activity and the position of the H-induced shape resonance as a function of support acidity/alkalinity in Pt/LTL catalysts. The analysis procedure allows the isolation of the shape resonance as induced by the chemisorption of hydrogen on the surface of the platinum particles. The fit of the shape resonance with a Fano-type line shape not only confirms the interpretation in terms of an antibonding resonance state, but also enables to determine the difference in energy of the AS state relative to the Fermi level.

The analysis method used is different in two aspects from procedures reported in the literature: (i) the edge alignment and (ii) the choice of reference spectrum as fully disussed in [24]. In previous work, either raw data were subtracted or all edges were aligned with the $L_{2,3}$ edges of platinum foil before subtraction. The alignment procedure based upon the absence (L_2) or presence (L_3) of electronic

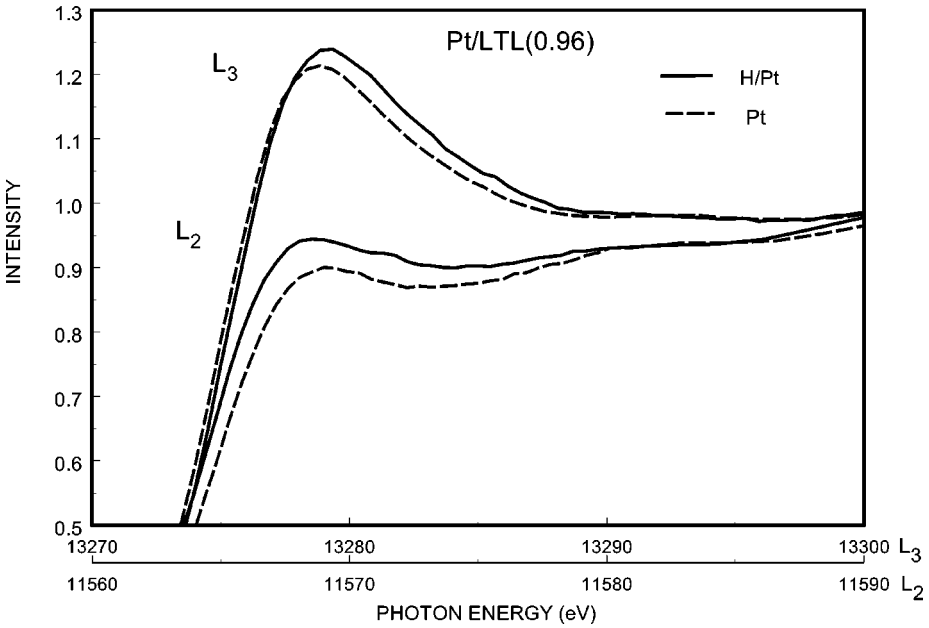

(a)

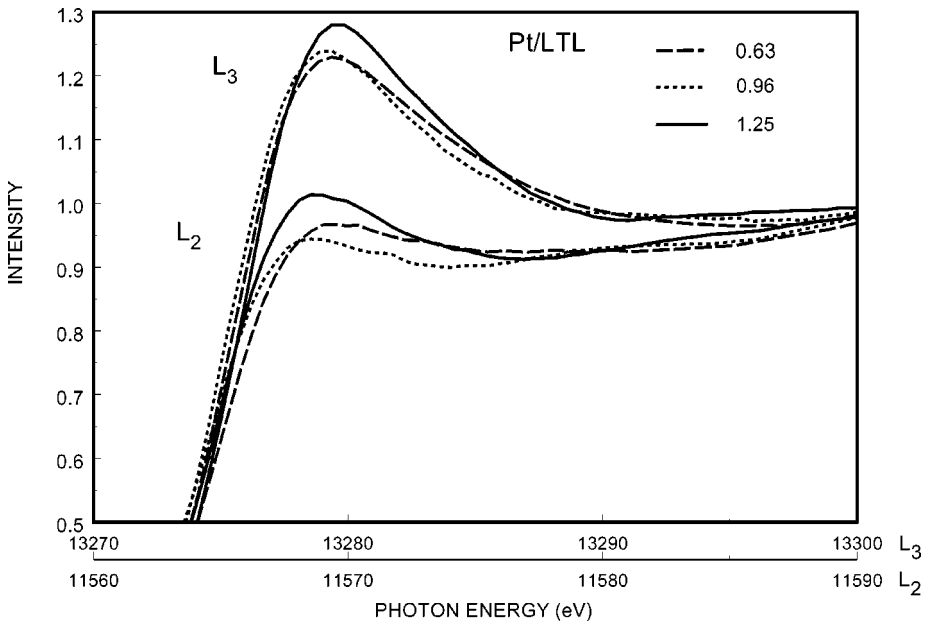

(b)

Figure 2. (a) L_3 and L_2 edges of Pt/LTL(0.96); solid line: chemisorbed hydrogen (H–Pt), dashed line: He treatment at 300 °C (Pt). (b) L_3 and L_2 edges of Pt/LTL with chemisorbed hydrogen; dashed line: K/Al = 0.63, dotted line: K/Al = 0.96, solid line: K/Al = 1.25.

structure (AS state) is critical to the success of the method. This alignment procedure is particularly suitable to study systems where much larger chemical shifts (initial state effects) are expected (e.g., large promoter and metal–support effects). Previously, a platinum foil spectrum was used as the reference in most work. However, this introduces both electronic and geometric contributions in the difference spectra due to the broader d-band and higher Pt–Pt coordination number of bulk platinum. Using the spectrum of the clean Pt cluster as a reference minimises the unwanted contributions in the spectra.

It should be pointed out that the differences between H–Pt and Pt are not a change in the unoccupied density of states due the chemisorption of hydrogen. A convincing argument for this is that the Fano profile of the Pt–H shape resonance does not change its shape, but only its amplitude with varying amounts of hydrogen coverage, as observed by Asakura et al. [21]. Such a systematic change in amplitude without a change in shape would not be expected if the differences were due to the change in density of states. The procedure of taking the direct difference with increasing amounts of hydrogen as applied by

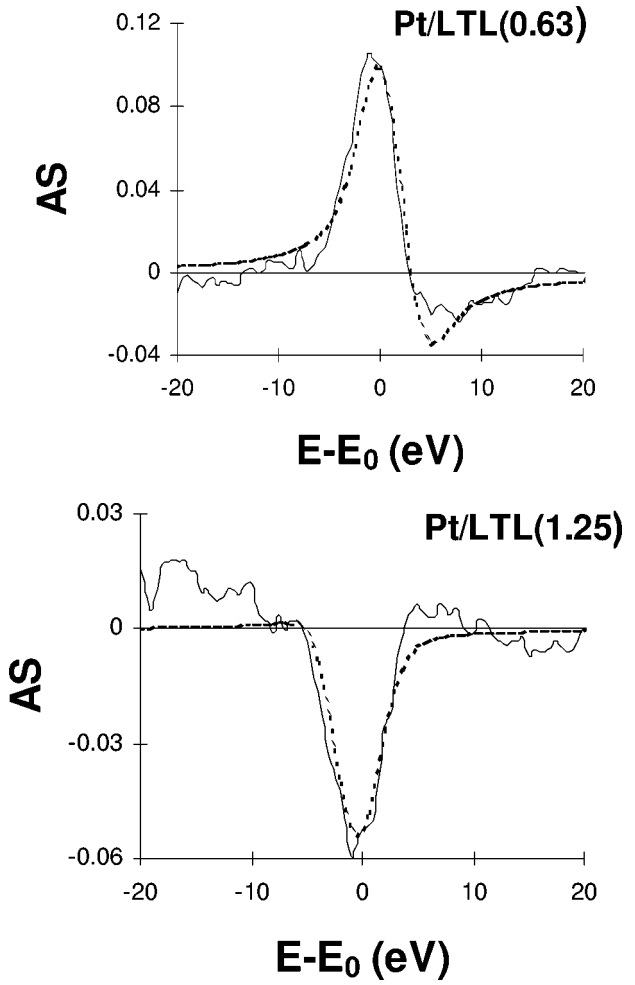

Figure 3. Pt–H antibonding shape resonance (AS) for Pt/LTL (0.63) and (1.25) (solid lines) and best fits (dotted lines) using equation (1) with the parameters as given in table 3.

Table 3
Fit parameters obtained from non-linear least squares fit of Fano-type line shape expression to the hydrogen-induced shape resonance in experimental spectra.[a]

Catalyst	A	E_{res}[b] (eV)	Width Γ (eV)	q
H–Pt/LTL(0.63)	0.15 ± 0.2	1.52 ± 0.1	1.86 ± 0.3	0.61
H–Pt/LTL(0.96)	0.07 ± 0.4	0.76 ± 0.1	1.16 ± 0.8	0.16
H–Pt/LTL(1.25)	0.06 ± 0.2	-0.99 ± 0.3	1.86 ± 0.9	-0.89

[a] $\alpha = -0.3$; $\beta = 0.6$ in $q = \alpha + \beta E_{\text{res}}$. Applied experimental width: Gaussian, 5 eV.
[b] Relative to the L_2 absorption edge.

Asakura et al. [21] is straightforward since only the amplitude of the AS and ΔXAFS (= Pt–H EXAFS) is changing. This simple method cannot be applied if the acidity/alkalinity (as in this work) and/or Pt particle size are different, since then the line shape of the AS and ΔVB are changing.

The present study towards metal–support effects demonstrates that the difference in energy of the antibonding state with respect to the Fermi level (E_{res}) decreases with increasing alkalinity of the LTL zeolite support. The q parameter, which is proportional to E_{res}, also shows the same effect. At the same time, the TOF of the neopentane hydrogenolysis reaction decreases several orders in magnitude with increasing alkalinity of the support (table 2). Since the neopentane hydrogenolysis is a monofunctional reaction catalysed by the metal [4,11,31,32], the results presented here can be discussed in terms of a direct influence of the support on the electronic structure of the platinum surface atoms thereby affecting their catalytic properties.

The decrease of E_{res} with increasing alkalinity of the LTL zeolite support implies a decrease in the strength of the Pt–H bond. These results are also in agreement with observations from XPS and FTIR spectroscopy. XPS showed a decrease of the Pd 3d orbital binding energy with increasing alkalinity. FTIR showed an enhanced metal to adsorbate CO π-backdonation with increasing alkalinity of the support. This results in a decrease of the linear to bridge bonded CO [33], which occurs due to a closer position (better overlap) of the donating d-orbital to the antibonding $2\pi^*$ CO orbital. A decrease in energy position (to lower binding energy) of the d-orbital interacting with the 1s orbital of hydrogen implies a larger energy difference between the two interacting orbitals, which according to MO theory leads to a weaker Pt–H bonding.

These results imply that the electronic structure of the platinum surface atoms is influenced by the support through a potential induced by the support and felt by the whole metal particle. The potential alters the energy position of the metal d-orbitals, which consequently changes the bonding properties of the platinum surface atoms. This has a direct influence on the catalytic properties of the metal particles. In forthcoming papers [30,34,35] we will show that direct information about the change in orbital energy position of the metal particles can be obtained from atomic XAFS. Even small changes in charge density (±0.02 electron) of the support-oxygen ions produce the effects without the need for electron transfer [35].

6. Conclusion

This study provides the most direct experimental evidence to date to support recently reported theoretical calculations concerning the nature of noble metal–atomic adsorbate bonding and its relationship to catalytic activity. This work is the first to demonstrate that the Pt–H resonance above the Fermi level can be observed, and that its energy and spectral line shape vary systematically with the alkalinity of the Pt cluster support. Generalisation to other metal–atomic adsorbate and, hopefully, even molecular bonding is anticipated. No measurement can more directly reflect the critical metal–adsorbate interaction, than observation of the bonding and antibonding orbitals constituting that interaction. The ability to watch the metal–adsorbate antibonding orbitals systematically vary with the alkalinity of

the support provides a major new tool for understanding the fundamental mechanism of the metal–support interaction and its effects on the electronic structure and activity of the catalysts.

References

[1] R.A. Della Betta and M. Boudart, in: *Proc. 5th Int. Congr. on Catal.*, ed. J.W. Hightower (North-Holland, Amsterdam, 1973) p. 1329.
[2] G. Larsen and G.L. Haller, Catal. Lett. 3 (1989) 103.
[3] A. de Mallmann and D. Barthomeuf, J. Chem. Phys. 87 (1990) 535.
[4] S.T. Homeyer, Z. Karpinski and W.M.H. Sachtler, J. Catal. 123 (1990) 60.
[5] W.M.H. Sachtler and A.Y. Stakheev, Catal. Today 12 (1992) 283.
[6] D.L. Shawn and M.A. Vannice, J. Catal. 143 (1993) 539.
[7] D.L. Shawn and M.A. Vannice, J. Catal. 143 (1993) 554.
[8] B.L. Mojet, M.J. Kappers, J.T Miller and D.C. Koningsberger, in: *11th Int. Congr. on Catal.*, Stud. Surf. Sci. Catal., Vol. 101B, eds. J.W. Hightower, W.N. Delgass, E. Iglesia and A.T. Bell (Elsevier, Amsterdam, 1996) p. 1165.
[9] Z. Zhang, T.T. Wong and W.M.H. Sachtler, J. Catal. 128 (1991) 131.
[10] A.Y. Stakheev and W.M.H. Sachtler, J. Chem. Soc. Faraday Trans. 87 (1991) 3703.
[11] G. Larsen and G.L. Haller, Catal. Today. 15 (1992) 431.
[12] A. de Mallmann and D. Barthomeuf, J. Chem. Phys. 87 (1990) 535.
[13] A. de Mallmann and D. Barthomeuf, Stud. Surf. Sci. Catal. 46 (1989) 429.
[14] A.P.J. Jansen and R.A. van Santen, J. Phys. Chem. 94 (1990) 6764.
[15] E. Sanchez-Marcos, A.P.J. Jansen and R.A. van Santen, Chem. Phys. Lett. 167 (1990) 399.
[16] A.N. Mansour, J.W. Cook, Jr. and D.E. Sayers, J. Phys. Chem. 96 (1992) 4690.
[17] F.W. Lytle, R.B. Greegor, E.C. Marques, V.A. Biebesheimer, D.R. Sandstrom, J.A. Horsley, G.H. Via and J.H. Sinfelt, ACS Symp. Ser. 288 (1985) 280.
[18] M.G. Samant and M. Boudart, J. Phys. Chem. 95 (1991) 4070.
[19] M. Vaarkamp, J.T. Miller, F.S. Modica and D.C. Koningsberger, J. Catal. 163 (1996) 294.
[20] A.V. Soldatov, S. Della Longa and A. Bianconi, Solid State Commun. 8 (1993) 863.
[21] K. Asakura, T. Kubota, N. Ichikuni and Y. Iwasawa, Stud. Surf. Sci. Catal. 101 (1996) 911.
[22] S.N. Reifsnyder, M.M. Otten, D.E. Sayers and H.H. Lamb, J. Phys. Chem. B 101 (1997) 4972.
[23] B.I. Boyanov and T.I. Morrison, J. Phys. Chem. 100 (1996) 16318.
[24] D.E. Ramaker, B.L. Mojet, M.T. Garriga Oostenbrink, J.T. Miller and D.C. Koningsberger, J. Phys. Chem. Chem. Phys. 1 (1999) 2293.
[25] B.L. Mojet, M.J. Kappers, J.C. Muijsers, J.W. Niemantsverdriet, J.T. Miller, F.S. Modica and D.C. Koningsberger, Stud. Surf. Sci. Catal. 84 (1994) 909.
[26] M. Vaarkamp, B.L. Mojet, F.S. Modica, J.T. Miller and D.C. Koningsberger, J. Phys. Chem. 99 (1995) 16067.
[27] J.W. Cook and D.E. Sayers, J. Appl. Phys. 52 (1991) 5024.
[28] B. Hammer and J.K. Nørskov, Nature 376 (1995) 238.
[29] B.L. Mojet, M.J. Kappers, J.T. Miller and D.C. Koningsberger, Stud. Surf. Sci. Catal. 101 (1996) 1165.
[30] B.L. Mojet, J.T. Miller, D.E. Ramaker and D.C. Koningsberger, J. Catal., in press.
[31] R.A. Dalla Betta and M. Boudart, in: *Proc. 5th Int. Congr. on Catal.*, ed. J.W. Hightower (North-Holland, Amsterdam, 1973) p. 1329.
[32] J.R. Anderson and N.R. Avery, J. Catal. 7 (1967) 315.
[33] R.A. van Santen, J. Chem. Soc. Faraday Trans. I 83 (1987) 1915.
[34] D.C. Koningsberger, J. de Graaf, B.L. Mojet, D.E. Ramaker and J.T. Miller, Appl. Catal., in press.
[35] D.E. Ramaker and D.C. Koningsberger, J. Catal., submitted.